Polyethylene/Grafted Polyethylene/Graphite Nanocomposites: Preparation, Structure, and Electrical Properties

Jing-Wei Shen, Wen-Yi Huang, Sheng-Wu Zuo, Jing Hou

College of Polymer Science and Engineering, Sichuan University, Chengdu 610065, China

Received 26 April 2004; accepted 2 October 2004
DOI 10.1002/app.21729
Published online in Wiley InterScience (www.interscience.wiley.com).

ABSTRACT: Polyethylene (PE)/maleic anhydride grafted PE (*g*-PE)/expanded graphite (EG) electrically conductive nanocomposites were successfully prepared by solution intercalation (SI) and masterbatch melt mixing (MMM). Electrical conductivity (σ) measurements; transmission electron, scanning electron, and optical miscroscopy observations; and differential scanning calorimetry analyses were employed to examine the influences of the preparation methods, EG volume or weight fractions (ϕ or f_w), and *g*-PE weight contents (C_g) on the structure and σ of the nanocomposites, as compared to PE/*g*-PE/EG composites and PE/EG control produced by direct melt mixing (DMM). The percolation thresholds (ϕ_c) of the SI, MMM, and DMM composites (C_g/f_w = 1.5) and the DMM control were measured and found to be 2.19, 3.81, 4.68, and 5.35%, respectively. As the C_g/f_w increases from 1 to 4, the σ of the MMM and DMM composites with f_w = 9% rises from the order of 10^{-16} to 10^{-4} and 10^{-8} S/cm, respectively. These were closely associated with the morphology and microstructure of the composites varying with the preparation methods (ϕ and C_g/f_w) and could also be interpreted in terms of percolation theory.
 J Appl Polym Sci 97: 51–59, 2005

Key words: nanocomposites; conducting polymers; morphology; polyethylene; graphite

INTRODUCTION

Polymer/graphite composites have found many significant applications in electrical or thermal conductors, electromagnetic interference shields, self-lubricated materials, and so forth.[1,2] Recently, much progress has been made in both polymer/layered silicate nanocomposites[3] and graphite intercalation compounds,[4] which in turn ignites an innovative idea for developing polymer/layered graphite composites. Graphite intercalation compounds have a layered structure composed of graphite flakes. Thus, once treated at a high temperature (>900°C), the graphite flakes would be expanded by several hundred times along their C axis. The nanometer-scale sheets and galleries[5] in the final expanded graphite (EG) as well as the hydroxyl and carboxyl groups[6] on the borders of sheets generated by chemical oxidation create favorable conditions allowing for suitable monomers, initiators, and even the macromolecules to intercalate and accordingly form polymer/EG nanocomposites.

In the past years, monomer-intercalated *in situ* polymerization was applied to fabricate polyamide-6/EG,[7] polystyrene/EG,[8,9] and poly(styrene-methylmethacrylate)/EG[10] nanocomposites. More recently, we prepared maleic anhydride grafted polypropylene (*g*-PP)/EG[11,12] and polypropylene (PP)/EG[13] nanocomposites using solution intercalation (SI) and masterbatch melt mixing (MMM). As far as the electrical conductivity is concerned, these materials exhibit a much lower volumic percolation threshold than the corresponding polymer/EG composites prepared by direct melt mixing (DMM), which indicates the tremendous potential and value of conducting nanocomposites. In the current work, we attempted to prepare polyethylene (PE)/EG nanocomposites through SI and MMM, as compared to the common composites obtained by DMM.

EXPERIMENTAL

Materials

Intercalated graphite (LX-2053) was obtained from Baoding Lianxing Carbide Co. with an average particle size of 0.30 mm and a density of 4 g/L and treated with a mixture of concentrated sulfuric acid and nitric acid (4:1, v/v). Nanjing Julong Chemical Co. supplied *g*-PE with a grafted ratio of 0.7–0.8 wt % and a melt index of 14 g/10 min. High-density PE (7006A) with a melt index of 6.5 g/10 min was produced by Qilu Petrochemical Co.

Correspondence to: J. Shen (jingwei_shen@163.com).
Contract grant sponsor: National Ministry of Education of China; contract grant number: 20010610031.

Sample preparation

The intercalated graphite was placed in an oven at 950 ± 10°C for rapid expansion (15 s) and exfoliation to obtain the EG. The resulting EG was dispersed in xylene to prepare a suspended solution with a certain EG content. The measured PE and *g*-PE were totally dissolved in xylene in a three-necked flask upon heating to reflux, and subsequently the EG suspended solution was added dropwise. After refluxing for 1.5 h, on cessation of heating, a portion of the xylene was extracted under a vaccum. When the temperature was decreased to about 60°C, the crude product was precipitated by acetone and then filtered and dried *in vacuo*. The resulting powder product was referred to as the SI compounds.

Following the above-described procedure, EG and *g*-PE were fabricated into a *g*-PE/EG masterbatch with a certain EG concentration, which was then blended with PE in the mixing chamber of a Haake System-40 torque rheometer (Haake Buchler Co.) at 190°C and 30 rpm for 8 min. The obtained lumpish compounds were denoted as MMM compounds. Under the same blending conditions, PE, *g*-PE, and EG were directly poured into the mixing chamber and blended; these clumpish compounds were named DMM compounds. The PE/EG control compounds were prepared using the DMM method and conditions.

These four kinds of compounds were compression molded at 190°C and 5 MPa for 3 min. This was followed by cooling at a holding pressure with a YX-50(D) semiautomatic press (Shanghai, China) to prepare plates with dimensions of 100 × 100 × 2 mm^3, which are denoted as the plates of SI, MMM, and DMM composites and PE/EG control.

Electrical conductivity measurements

The volume conductivity (σ) of the plate samples was measured at room temperature with a ZC36 high-resistance meter (Shanghai Precise Instrument & Meter Co., China) when the σ was less than 10^{-8} S/cm or with a DT9205 numeric multimeter (Shenzhen Zhongjia Instrument & Meter Co.) when the σ was greater than 10^{-8} S/cm. In the latter case, pieces of copper foil fastened with a conducting paste were used as the electrodes. Data were recorded at 10 s after applying the voltage.

Transmission electron microscopy (TEM) observation

A TE microscope (JEM-100CX II, Kyoto, Japan) was used to observe the microstructure of the EG particles in the composites. Ultrathin samples were obtained by microtoming the frozen plates using an LKB V ultramicrotome (LKB Ultrascan XL, Bromma, Sweden), equipped with a freezing chamber.

Scanning electron microscopy (SEM) observation

An SE microscope (Hitachi X-650, Japan) was employed to observe the microscopic structure of EG and the composites. The plate samples were freeze-fractured, and the fractured surfaces were gold sputtered under a vacuum.

Optical microscopy (OM) observation

An OM microscope (Leitz Diaplan, Wetzlar, Germany) was applied to observe the dispersed morphology of EG particles in the composites. Upon employing the reflected lights, samples with a thickness of 0.5 mm were obtained by slicing the plates along the direction of thickness. In the case of applying transmitted lights, a thin sample (6 μm) was prepared by cutting the liquid nitrogen frozen plates using a Leica microtome. During observation, the contrast ratio of the visual field was adjusted by regulating the rotation angle of the polarizing prism in order to gain clear pictures, which were recorded by a microcomputer numeric picture-processing system.

Differential scanning calorimetry (DSC) analyses

A DSC calorimeter (Perkin Elmer Pyris 1) was employed to examine the nonisothermal crystallization characteristics of the composites. They were first heated to 190°C and held there for 10 min, and then they were cooled to room temperature at a rate of 10°C/min in an N_2 atmosphere.

RESULTS AND DISCUSSION

Effect of EG content on structure and conductibility of composites

Relationship between conductivity and EG content

Figure 1 shows the relationship between the electrical conductivity (σ) and EG volume fraction (ϕ) for the SI, MMM, and DMM composites with a constant weight ratio (R_w = 1.5) of *g*-PE to EG, and the PE/EG control. When ϕ was calculated from the EG weight fraction (f_w), the solid densities of EG, PE, and *g*-PE were taken as 2.26,[12] 0.95, and 0.90 g/cm^3 (measured values), respectively. The inset of Figure 1 represents the plot of $d\sigma/d\phi$ versus ϕ. The corresponding ϕ to its peak value was set as the percolation threshold (ϕ_c).[14] The ϕ_c values of SI, MMM, and DMM composites and PE/EG control are 2.19, 3.81, 4.68, and 5.35%, respectively. The ϕ_c values of the first three composites decreased by about 60, 30, and 13%, respectively, in comparison to that of the PE/EG control.

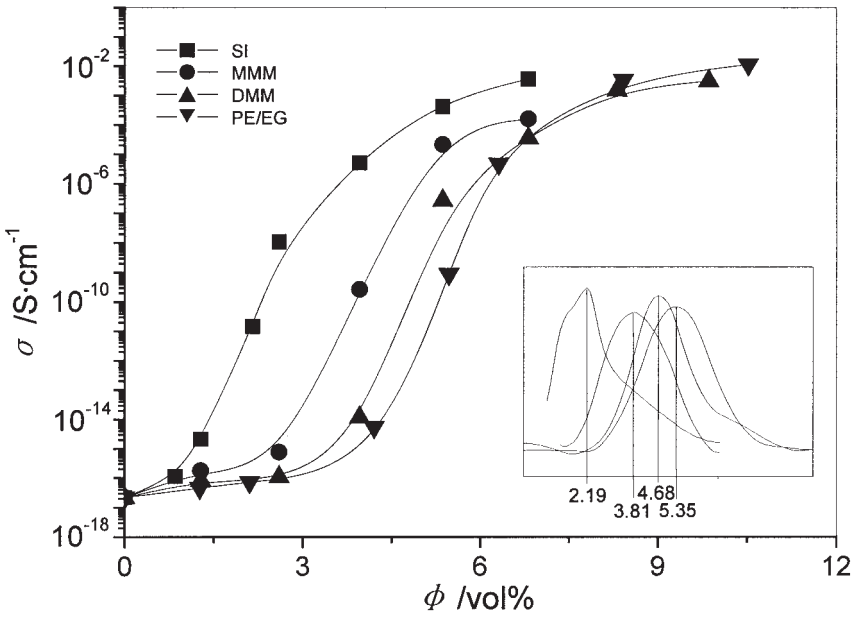

Figure 1 The electrical conductivity (σ) versus the EG volume fraction (ϕ) for SI, MMM_s and DMM composites with a weight ratio of g-PE to EG (R_w) of 1.5 and DMM PE/EG control.

Morphology and microstructure of EG dispersed phase

Figure 2 gives TEM photographs of SI and MMM composites with $\phi = 3.96\%$ and $R_w = 1.5$. The black lines and white domains are referred to as the EG sheets and the polymers, respectively. In SI composites [Fig. 2(a,b)], it can be repeatedly observed that the graphite nanosheets with thickness and interlayer spacing of about 10 nm, and high aspect (width to thickness) ratio of more than 30, parallel each other. This indicates that the graphite nanosheets in EG have constructed a nanocomposite structure with the polymers. With regard to MMM composites [Fig. 2(c)], most of the graphite sheets are parallel to each other, but their thickness and interlayer spacing are nonuniform with the reduced aspect ratios. This means that, despite the formation of a nanocomposite structure in MMM composites, its regularity has largely decreased. For DMM composites (not shown), except in local domains, poorly regular nanostructures exist, most of graphite aggregates in the form of bundles.

Figure 3 shows SEM micrographs of EG and the SI, MMM, and DMM composites. On the scale of 10s of microns, EG has a network structure comprising many graphite sheets with thicknesses of about 50–80 nm[9] and pores ranging from 10 nm to 10 μm,[5] as indicated

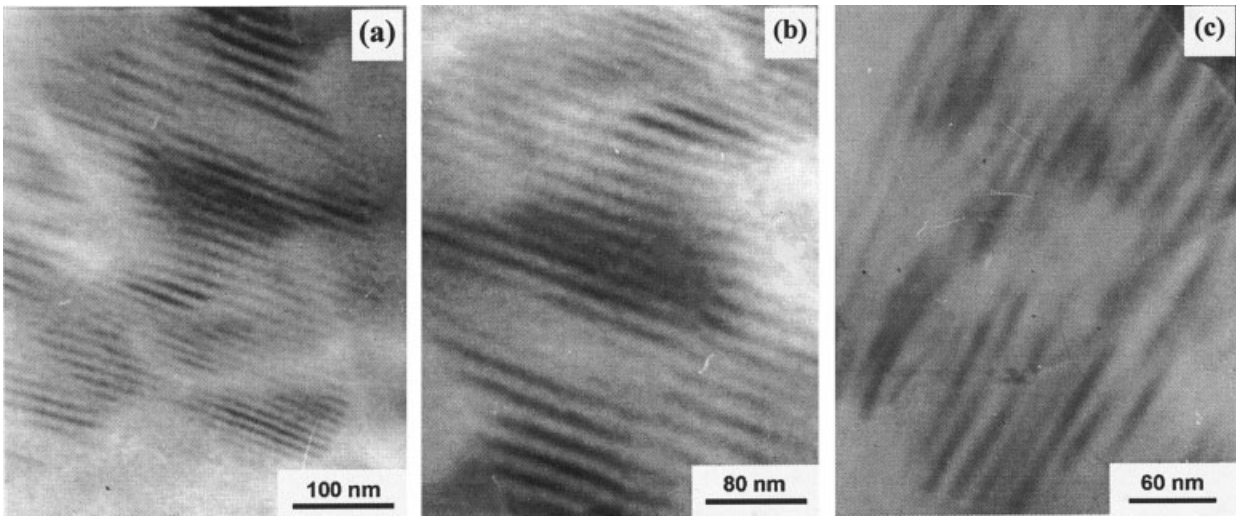

Figure 2 TEM micrographs of the composites with $\phi = 3.96\%$ and $R_w = 1.5$ prepared by (a,b) SI and (c) MMM.

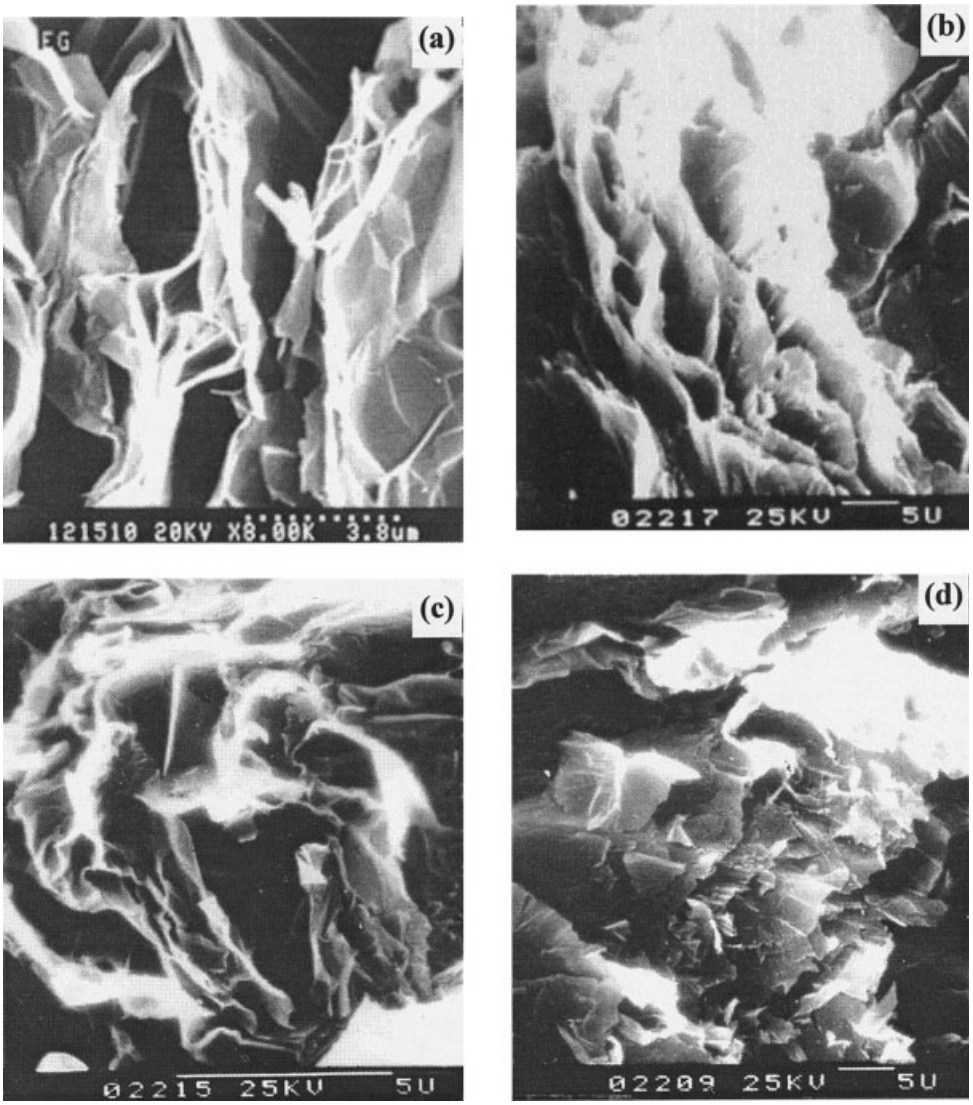

Figure 3 SEM micrographs of (a) EG and the composites with $\phi = 3.96\%$ and $R_w = 1.5$ prepared by three methods. (b) SI, (c) MMM, and (d) DMM.

in Figure 3(a). In SI composites [Fig. 3(b)], the original network structure of EG has been essentially retained, which indicates that the graphite sheets of EG have constructed a micron composite network with the polymers. In MMM composites [Fig. 3(c)], the original sheet network of EG has deformed to a larger extent, which means that the structure regularity of the formed EG–polymer micron composite network has decreased. As for DMM composites [Fig. 3(d)], the graphite sheets have been seriously collapsed and broken, and the EG–polymer micron composite network has almost been destroyed.

The reflected and transmitted OM photographs show the differences in the EG particle dispersed morphology of SI, MMM, and DMM composites, as indicated in Figure 4. It can be found that on the scale of 100s of microns, the size, aspect ratio, and occupied volume of EG particles are the largest in the SI composites [Fig. 4(a,d)], followed by the MMM composites [Fig. 4(b,e)], and the smallest in DMM composites [Fig. 4(c,f)]. This suggests that for different preparation methods, not only does the internal microstructure of EG particles in the composites change, but also differences exist in their sizes, aspect ratios, and occupied volumes. Hence, there must be an intrinsic correlation among them. The TEM, SEM, and OM observations mentioned above characterized the microstructure and morphology of PE/*g*-PE/EG composites with $\phi = 3.96\%$ and $R_w = 1.5$ from three different scales, which is consistent with the results of our previous work on PP/*g*-PP/EG composites.[13] The reasons why different preparation methods cause the structural and morphological changes of these composites on three different scales have been elaborated in the literature,[11–13] without the necessity to reiterate here. It should be emphasized that for the composites with the

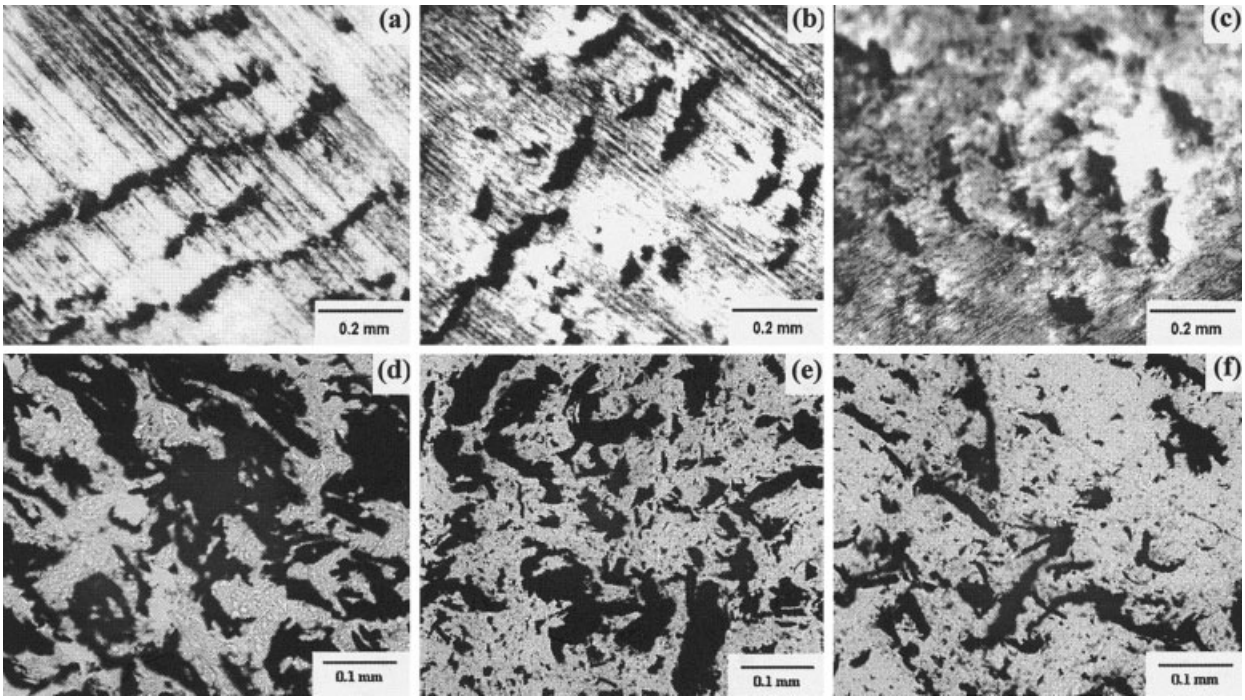

Figure 4 (a–c) Reflected and (d–f) transmitted OM photographs for the composites with $\phi = 3.96\%$ and $R_w = 1.5$ prepared by three methods: (a,d) SI, (b,e) MMM, and (c,f) DMM.

same composition but obtained from different preparation methods, the size, aspect ratio, and internal structure regularity of EG particles are drastically dependent on two factors associated with preparation methods. The first one is the extent of shearing exerted on materials, which is due to the fact that although EG itself can endure large compression stress, it is ready to be fragmented in the course of shearing.[15] The second factor is the filled degree of polymer in the EG particles, because the EG particles internally supported by polymers can boost the resistance to break up.

DSC data supplement and authenticate the structural and morphological results characterized above. It can be seen in Table I that in contrast to the PE/EG control with $f_w = 9\%$, the crystallization onset temperature ($T_{c,o}$) and especially the crystallization peak temperature ($T_{c,p}$) are regularly shifted to lower temperatures for SI, MMM, and DMM composites with $f_w = 9\%$ and $R_w = 1.5$, which means that the effect of EG on the heterogeneous nucleation of PE and *g*-PE crystallization successively decreases. The difference between the two characteristic temperature ($T_{c,o} - T_{c,p}$) increases in the sequence of SI, MMM, and DMM composites, which verifies that the crystallization rate decreases in the proper order, are due to the sequentially increased obstruction of EG on the crystallization of *g*-PE and PE, arising from the existence of physical adsorption and polar interaction between the borders of the graphite sheets and intercalated polymers, especially *g*-PE. This implies that as the amount of polymers intercalated into the EG interior increases, the structural regularity of the EG–polymer composite network within the EG particles as well as their sizes and aspect ratios gradually rise. The crystallization enthalpy (ΔH_c) associated with crystallinity is reduced, which is the combined consequence of the influenced nucleation and crystallization rate and further substantiates the rationality of the above analyses.

Influencing mechanism

The prerequisite condition for transforming polymer/conductive filler composites into electrical conductors is the formation of conducting paths arising from the adjacency or contacts of filler particles. Therefore, for the composites with the same ϕ of fillers, filled particles with larger size and aspect ratio are much easier to form conducting paths than the reverse case; in turn, the corresponding composites exhibit σ. In other

TABLE I
DSC data under Cooling Procedure for Composites ($f_w = 9\%$, $R_w = 1.5$) Prepared by Three Methods and DMM-PE/EG Control ($f_w = 9\%$)

Preparation methods	SI	MMM	DMM	PE/EG
$T_{c,o}$ (°C)	123.46	121.68	121.34	124.28
$T_{c,p}$ (°C)	114.74	114.69	115.42	118.22
($T_{c,o} - T_{c,p}$) (°C)	8.72	6.99	5.92	6.06
ΔH_c (Jg^{-1})	−111.77	−118.35	−119.62	−126.37

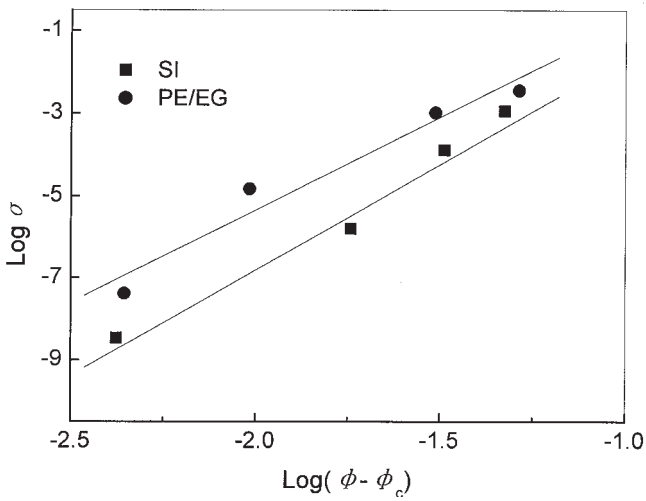

Figure 5 A plot of log σ versus log($\phi - \phi_c$) for the SI composite with $R_w = 1.5$ and the DMM PE/EG control.

words, the ϕ value corresponding to the formation of conducting paths in the composites with larger size and aspect ratio of particles is lower than that of the reverse case, namely, a lower ϕ_c. This is the primary cause of the conductibility of SI, MMM, and DMM composites with different EG particle morphology and microstructures being remarkably different from each other.

Percolation theory[16,17] can be employed to explain the insulator–conductor transition occurring in the composite systems when a critical ϕ of conducting fillers is reached, using the following equation:

$$\sigma = \sigma_0(\phi - \phi_c)^u \quad (1)$$

where u is a critical exponent of conductivity, which depends only on the dimensionality of the systems.

Figure 5 gives the plot of logσ versus log($\phi - \phi_c$) for the SI composite with $R_w = 1.5$ and the PE/EG control. The u values can be determined from the slopes of the straight lines in Figure 5. Table II lists the u values for the four composites, appended with the correlation coefficients (R) for linear fitting. It is obvious that the σ–ϕ relationships for these composites can be described in terms of the percolation equation, but the u value lies approximately between 4.5 and 5.2, which is greater than the average field universal value ($u = 3$)[18] for the statistical percolation lattice model.

TABLE II
Critical Exponents of Composites ($R_w = 1.5$) Prepared by Three Methods and DMM PE/EG Control

Preparation method	u	R
SI	5.223 ± 0.490	0.991
MMM	4.815 ± 0.414	0.993
DMM	4.545 ± 0.319	0.998
PE/EG	4.500 ± 0.687	0.977

TABLE III
Relationship Between Electrical Conductivity (σ) and g-PE Weight Content (C_g) or R_w for Composites (f_w = 9%) Prepared by Two Methods

		σ (S cm^{-1})	
R_w	C_g (%)	MMM	DMM
0	0	3.4×10^{-16}	3.4×10^{-16}
1	9	9.5×10^{-16}	7.1×10^{-16}
1.5	13.5	5.7×10^{-14}	9.8×10^{-16}
2	18	8.8×10^{-12}	5.4×10^{-15}
3	27	1.5×10^{-5}	2.1×10^{-9}
4	36	1.1×10^{-4}	1.2×10^{-8}
5	45	5.8×10^{-4}	2.9×10^{-8}

Effect of g-PE content on morphology and conductibility of composites

Relationship between conductivity and g-PE content

Table III shows the σ varying with the C_g for MMM and DMM composites at a given EG weight fraction ($f_w = 9\%$). Because $C_g \leq 9\%$ ($R_w \leq 1$), the σ values for these two composites and their difference are very small, and the σ values are both on the order of 10^{-16} S/cm. When the C_g values of MMM and DMM composites are larger than 9 ($R_w > 1$) and 18% ($R_w > 2$), respectively, the σ increases by several orders of magnitude; when $C_g \geq 27\%$ ($R_w \geq 3$), the σ levels off and reaches the order of 10^{-4} and 10^{-8} S/cm, respectively. Surprisingly, for MMM and DMM composites with $f_w = 9\%$, the enhancement of σ due to the increase of C_g or R_w arrives at 12 and 8 orders of magnitude, respectively.

Morphology of EG dispersed phase

The morphological differences of EG particles in MMM and DMM composites with $f_w = 9\%$ ($\phi = 3.96\%$) and $C_g = 13.5\%$ ($R_w = 1.5$) is represented in Figure 4. As shown in Figure 6, the reflected and transmitted OM photographs illustrate the morphological difference between these two composites with $f_w = 9\%$ and $C_g = 27\%$ ($R_w = 3$). It can be seen that at the same C_g or R_w, the size, aspect ratio, and occupied volume of EG particles in MMM composites are superior to those in DMM composites. In addition, with regard to the same preparation method, the size, aspect ratio, and occupied volume of EG particles in the composites with $C_g = 27\%$ ($R_w = 3$) are larger than those in the composites with $C_g = 9\%$ ($R_w = 1.5$). This can be interpreted as follows.

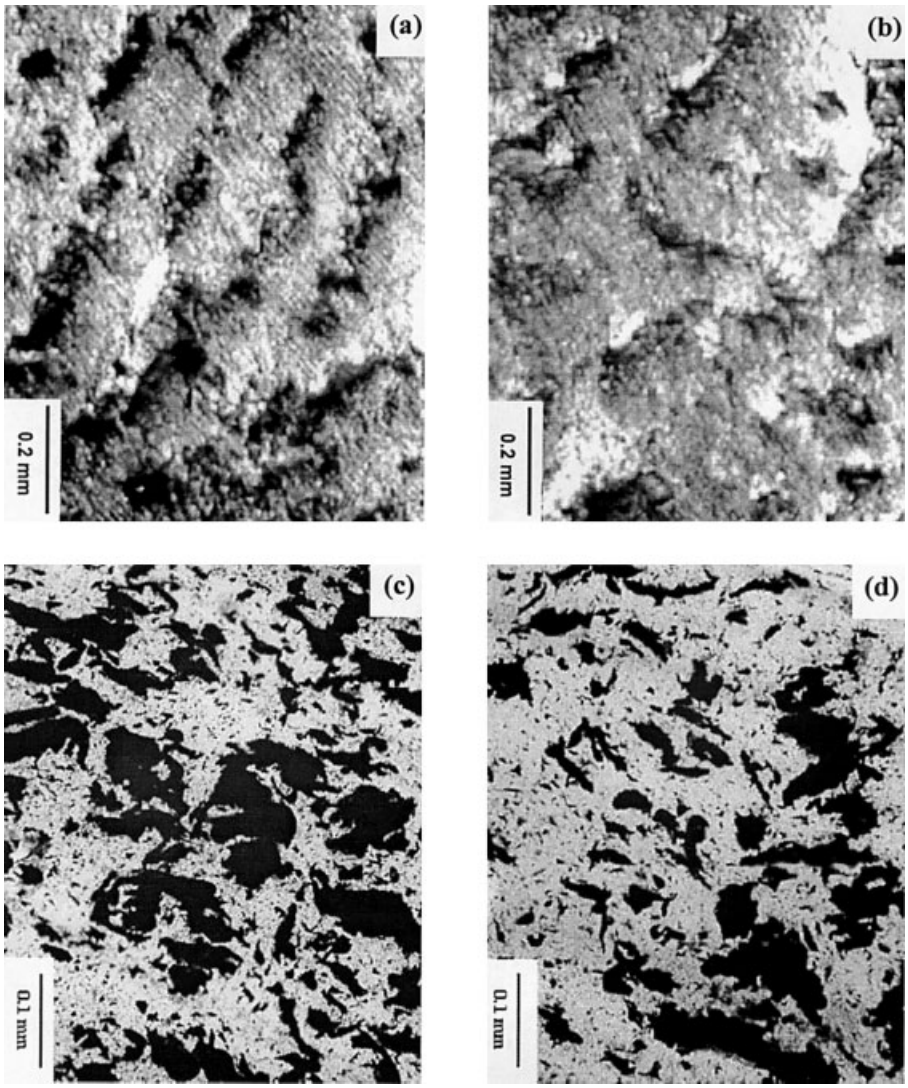

Figure 6 (a,b) Reflected and (c,d) transmitted OM photographs for the composites with f_w = 9% and R_w = 3 prepared by (a,c) MMM and (b,d) DMM.

When MMM and DMM composites with the same composition are prepared, although the materials are subjected to the same shearing during melt mixing, the extent of destroyed EG particles in MMM composites is smaller than that in DMM composites, because the resistance to shear fragmentation of EG particles in the former is enhanced by the support of intercalated *g*-PE, which is attributable to the application of a *g*-PE/EG masterbatch prepared by the SI method. As a result, the size, aspect ratio, and occupied volume of EG particles in MMM composites are larger than those in DMM composites.

When the same preparation method is used to obtain the composites with the same f_w but different C_g or R_w values, in the case of higher C_g or R_w, the amount of polymers (mainly *g*-PE) intercalated into EG particles is larger than that in the reverse case, because the molecular weight of *g*-PE is lower than PE (i.e. low viscosity of *g*-PE), and especially its molecular polarity is much higher than that of PE. (There is a stronger interaction between polar *g*-PE molecules and polar groups[6] on the borders of EG graphite sheets.) Therefore, in the former case, the resistance to shear fragmentation of EG particles is greater than that of the latter. Thus, under the same processing conditions the higher C_g or R_w leads to larger size, aspect ratio, and occupied volume of EG particles in the composites.

Influencing mechanism

The relationship between σ and C_g or R_w for MMM and DMM composites with f_w = 9% represented in Table III can be interpreted in terms of the formation mechanisms of conducting paths according to percolation theory, which is associated with the variation of

the morphology with the preparation methods and C_g or R_w.

When $C_g \leq 9\%$ ($R_w \leq 1$), the size, aspect ratio. and occupied volume of EG particles in the two composites are very small; then, the distance between particles is too large to form conducting paths. Thus, a low σ value on the order of 10^{-16} S/cm for these composites seems reasonable. As the C_g values of MMM and DMM composites increase up to 9 ($R_w > 1$) and 18% ($R_w > 2$), respectively, the size, aspect ratio, and occupied volume of the EG particles are greatly enlarged, and the distance between particles becomes small enough to initiate the formation of conducting paths. Consequently, the σ of the composites begins to climb. Because at the same C_g or R_w value the size, aspect ratio, and occupied volume of EG particles in MMM composites are larger than those of DMM composites (see Fig. 4, $C_g = 13.5\%$ and $R_w = 1.5$), the former can start to produce conducting paths at lower C_g or R_w than the latter. As $C_g \geq 27\%$ ($R_w \geq 3$), the size, aspect ratio, and occupied volume of EG particles in the two composites become large enough to construct the conducting path network engendered by adjacency or contact of particles, then the σ values of the composites tend to reach their individual utmost values. Furthermore, because at the same C_g or R_w value the size, aspect ratio, and occupied volume of EG particles in MMM composites are always larger than those of DMM composites (see Fig. 6, $C_g = 27\%$ and $R_w = 3$), the perfection of conducting path networks in the former is superior to that in the latter. Accordingly, the σ of the former arrives at a value on the order of 10^{-4} S/cm, which is greater by 4 orders of magnitude than the latter.

In view of the similar features observed in PP/*g*-PP/EG composites with $f_w = 9\%$ prepared by the MMM method,[13] it can be said that this kind of phenomenon is not fortuitous but pervasive. It implies that for certain conducting composites made up of polymer blends and conducting fillers, not only does the increase of filler concentration (ϕ or f_w) induce percolation effect, facilitating the σ of composites climbing and leveling off, but also at a given ϕ or f_w, the increase of certain component polymer concentrations (C_g) will result in similar percolation effects, requiring that the addition of this component polymer enhance the size, aspect ratio, and occupied volume of filler particles. (The structure regularity within particles will be improved simultaneously.) It should be pointed out that this kind of effect is quite distinguished from the concept and principle of double percolation.[19] Here, we did not employ the selective localization of conductive fillers (i.e., carbon black) in one phase or at the interface of polymer blends to generate double percolation in order to improve the conductibility of composites; but, in a particular way, suitable macromolecules are incorporated into the composites for facilitating the formation of a regular nanocomposite structure in the interior of the EG particles and microcomposite network, in turn raising the size and aspect ratio of the EG particles. Consequently, the effective occupied volume of conductive particles is dramatically enlarged, which results in the reduced amount of fillers required for the formation of conducting networks (i.e., low ϕ_c). As differentiated from double percolation, this effect should be defined as compounded particle percolation.

CONCLUSIONS

Through incorporation of *g*-PE, PE/EG nanocomposites can be prepared by SI and MMM methods. Under the given processing conditions, the ϕ_c values of SI, MMM, and DMM composites with $R_w = 1.5$ are reduced by 60, 30, and 13%, respectively, as compared to that of the PE/EG control. This can be ascribed to the fact that at the same ϕ, the structural regularity of the EG–polymer nanocomposite structure and microncomposite network within the EG particles, their size, and their aspect ratio decrease in sequence; whereas the amount of polymers (mainly *g*-PE) intercalated into EG particles depends on preparation methods and the extent of fragmentation of EG particles relies on the degree of shearing during the preparation of composites.

The σ values of MMM and DMM composites with $f_w = 9\%$ are associated with R_w, and the σ–R_w relationship at the given f_w exhibits a percolation feature similar to the σ–ϕ relationship at a constant R_w. When R_w increases from 1 to 4, the σ values of SI and MMM composites are raised from the order of 10^{-16} to 10^{-4} and 10^{-8} S/cm, respectively, which arises from the increased size and aspect ratio of EG particles attributable to the increment of *g*-PE contents, especially for MMM composites.

The σ–ϕ relationship at $R_w = 1.5$ and the σ–R_w relationship at $f_w = 9\%$ for the composites prepared by different methods can be interpreted through the formation mechanism of conducting paths according to percolation theory, associated with the morphological changes in the composites. The σ– relationship at $R_w = 1.5$ can be described using the percolation equation. The obtained critical exponential u is between nearly 4.5 and 5.2, which is larger than the average field universal value ($u = 3$) of the statistical percolation lattice model.

The authors gratefully acknowledge the support of the Doctoral Research Foundation granted by the National Ministry of Education of China. Special thanks are also due to the State Key Laboratory of Polymer Materials Engineering, Sichuan University, for the structural characterizations.

References

1. Foy, J. V.; Lindt, J. T. Polym Compos 1987, 8, 419.
2. Ponomarenko, A. T.; Shevechenko, V. G.; Enikolopyan, N. S. Adv Polym Sci 1990, 96, 125.
3. Christopher, O. O. J Chem Ed 2000, 77, 1138.
4. Herold, C.; Herold, A.; Lagrange, P. J. Phys Chem Solid 1996, 57, 655.
5. Cao, N. Z.; Shen, W. C.; Wen, S. Z.; Zhao, A. New Carbon Mater 1995, 11, 51.
6. Kotov, N. A.; Dékány, I.; Fendler, J. H. Adv Mater 1996, 8, 637.
7. Pan, Y. X.; Yu, Z. Z.; Ou, Y. C.; Hu, G. H. J Polym Sci Part B: Polym Phys 2000, 38, 1626.
8. Xiao, P.; Xiao, M.; Gong, K. C. Polymer 2001, 42, 4813.
9. Chen, G.; Weng, W.; Wu, D.; Chen, J.; Ye, L.; Yan, W. Acta Polym Sin 2001, 19, 803.
10. Yi, X. S.; Song, Y. H.; Zhen, Q. J Appl Polym Sci 2000, 77, 792.
11. Shen, J. W.; Chen, X. M.; Huang, W. Y. J Appl Polym Sci 2003, 88, 1864.
12. Chen, X. M.; Shen, J. W. Acta Polym Sin 2002, 20, 331.
13. Quan, C. Z.; Shen, J. W.; Chen, X. M. Acta Polym Sin 2003, 6, 831.
14. Deleuze, C.; Dufort, M.; Furdin, G.; Marêché, J. F.; McRae, E.; Celzard, A. J Phys Chem Solids 1996, 57, 715.
15. Wan, Y. S.; O'Gurkis, M. A.; Lindt, J. T. Polym Compos 1986, 7, 349.
16. Kirkpatrick, S. Phys Rev Lett 1971, 27, 1722.
17. Stuffer, D.; Aharony, A. Introduction to Percolation Theory; Taylor & Francis: London, 1985.
18. Heaney, M. B. Phys A 1997, 241, 296.
19. Gubbles, F.; Blacher, S.; Vanlathem, E.; Jerome, R.; Deltour, R.; Brouers, F.; Teyssie, Ph. Macromolecules 1995, 28, 1559.